Indian Journal of Chemistry
Vol. 56A, December 2017, pp. 1321-1326

Preparation and catalytic property of carbon nanotubes supported Pt and Ru nanoparticles for hydrogenation of aldehyde and substituted acetophenone in water

Zhiwang Yang*, Cheng Lei, Wenlong Chen, Ruxue Liu, Hong Wei, Yali Ma, Shuangyan Meng, Shaoping Hu & Yuli Wei

Key Laboratory of Polymer Materials of Gansu Province, Key Laboratory of Eco-Environment-Related Polymer Materials, Ministry of Education, College of Chemistry and Chemical Engineering, Northwest Normal University Lanzhou 730070, China

Email: yangzw_nwnu@163.com

Received 16 September 2017; revised and accepted 30 November 2017

Pt and Ru nanoparticles are deposited on carbon nanotubes via a simple wet impregnation method using aqueous solutions of platinum and ruthenium salts to prepare the supported catalysts of Pt/CNTs (nominal load 5 wt%) and Ru/CNTs (nominal load 10 wt%). The catalysts are characterized by XRD, XPS, BET and TEM data and tested for the hydrogenation of aldehyde and substituted acetophenone using pure water as the sole solvent. The reaction conditions are well optimized through the hydrogenation of *p*-methoxybenzaldehyde and acetophenone. These catalysts exhibit high activity for the hydrogenation of aldehydes and ketones. Many aldehydes and ketones can be efficiently converted to the corresponding alcohols in the presence of Pt/CNTs and Ru/CNTs. The use of water as solvent makes this catalytic system environmental-friendly.

Keywords: Catalytic hydrogenation, Hydrogenation, Carbon nanotubes, Nanoparticles, Platinum, Ruthenium, Aldehydes, Ketones, Wet impregnation method

Since green chemistry's emergence as an environmental friendly field in early 1990s[1], there has been a renewed interest in the age-old pursuit of the organic chemist to design and successfully apply the ideal synthesis in terms of efficiency, with atom[2-4] and step economy[4] being a major goal. The area of environmentally benign solvents has been one of the leading research areas of green chemistry with significant advances seen in aqueous (biphase) catalysis[5, 6] and the use of supercritical fluids[7] in chemical reactions. Ionic liquids[8, 9] and fluorous media[10] have also been used as green solvents.

Water bears unique characteristics that differ from the other solvents; it is cheap, most abundant in nature, and proven to have some unexpected beneficial effects in organic transformations.[11-13] Sharpless *et al.*[14] demonstrated the benefits of carrying out C-C bond-formation reactions "on water". Xiao *et al.*[15, 16] discovered that water is an excellent solvent for the asymmetric transfer hydrogenation of ketones. Good results were reported for reactions of acetophenone in water by Eichenseer *et al.*[17]

Several homogeneous catalytic hydrogenation processes are reported in the literature for the reduction of aldehydes.[18-23] However, in most cases catalyst recovery and product isolation were cumbersome. Therefore, heterogeneous catalyst became a better choice with more than 90% of the chemical manufacturing industries using catalysis in at least one step of the processes because of the intrinsic characteristics such as porosity and surface area which play a crucial role in the catalytic performances.[24]

CNTs have potential applications in a wide variety of areas because of their unique quasi-one-dimensional structural features, high specific surface area, high conductivity, and electrochemical stability.[25-32] Application of CNTs as catalysts and/or catalyst supports have been reported. Oxygen-containing surface groups were introduced in the CNTs by treatment with conc. nitric acid,[33] and hence the CNTs-based catalysts could disperse in water efficiently.

In the present study, Pt and Ru nanoparticles were deposited on carbon nanotubes via a simple wet impregnation method using aqueous solutions of platinum and ruthenium salts and tested for the hydrogenation of aldehyde and substituted acetophenone using pure water as the sole solvent. These catalysts exhibited high activity for the hydrogenation of aldehydes and ketones. The use of water as solvent makes this catalytic system environmental-friendly.

Experimental

CNTs were treated with aqueous HNO_3 solution following a procedure adapted from the literature[34]. Briefly, 2 g of CNTs were suspended in 100 mL of conc. HNO_3 (68 wt%) and refluxed at 140 °C in an oil bath for 14 h. After the mixture was cooled down to room temperature, it was filtered and washed with deionized water until the pH of the filtrate was around 7. Then the product, carbon nanotubes with open ends

and no other metal residuals, was dried in vacuum at 50 °C for 18 h.

The Pt/CNTs catalyst with nominal load of 5 wt% Pt loadings was prepared according to a previously published procedure[35, 36]. Briefly, The CNTs (1.0 g) with open ends were immersed in an aqueous solution of H_2PtCl_6 (25 mL, 10.27 mmol L^{-1}) at room temperature. After ultrasonic treatment for 3 h, the mixture was stirred for 48 h at room temperature. The mixture were then reduced by adding a 0.3 *M* aqueous solution of $NaBH_4$ dropwise (molar ratio of BH_4^-/Pt^{4+}= 20), and the resulting solid product was filtered, washed with deionized water, and dried at 60 °C for 18 h.

For the preparation of the Ru/CNTs catalyst with nominal load of 10 wt% Ru loadings, the pretreated CNTs (1.0 g) were immersed in an aqueous solution of $RuCl_3 \cdot xH_2O$ (25 mL, 53.03 mmol L^{-1}) at room temperature. After ultrasonic treatment as above and stirring, the mixture was reduced by adding a 1.5 *M* aqueous solution of $NaBH_4$ dropwise (molar ratio of BH_4^-/Ru^{3+}= 20). The resulting solid product was filtered, washed with deionized water, and dried at 60 °C for 18 h.

The catalysts were characterized by Fourier transform-infrared spectroscopy (FT-IR) on a Nicolet NEXUS 670 spectrometer using KBr disks in the scanning range of 4000-400 cm^{-1}. Transmission electron microscope (TEM) measurements were made by a JEOL 2010 microscope. The BET-nitrogen isotherms were used to quantify changes in the specific surface area using an ASAP 2020 specific surface area and pore size analyzer. The X-ray diffractometer (XRD, D/max-2400) was used for identifying platinum oxides as well as their oxidation states on the outer and inner surfaces of the carbon nanotubes. An XPS instrument (Thermo VG Scientific Sigma Probe) using an Al-K_α radiation was used to study the surface compositions of the catalysts. The oxidation product was identified through gas chromatograph (GC) analyses on a Shimadzu GC-2010 equipped with a 25 m×0.25 mm SE-54 column and a FID detector.

The experiments on catalytic activity were carried out in a 50 mL stainless steel autoclave with a magnetic stirrer, with distilled water as the sole solvent. The conditions for aldehyde hydrogenation reaction with Pt/CNTs catalyst were as follows: 1 mmol of aldehyde, 0.01 g catalyst and 3 mL of water were taken in the autoclave. The pressure of H_2 was maintained 3.0 MPa before five times displacing of air from the autoclave. The catalytic system was then stirred at the rate of 600 rpm at 30 °C for a set time. The selectivity and conversion were calculated with an external normalization method by GC analysis. The ketone hydrogenation reaction was carried out with Ru/CNTs catalyst similarly under the following conditions: 0.9 mmol of ketone, 0.01 g catalyst and 3 mL of water.

The hydrogenation activity of the is expressed by the average turnover frequency (TOF), and calculated based on the total number of metal atoms on the catalyst. The conversion used to calculate the TOF was lower than 30%.

Results and discussion

The morphology, size, and dispersion of Pt nanoparticles were examined by TEM. It can be seen from Fig. 1 that the tubular structure of the multi-walled carbon nanotubes remains fairly intact even during the pretreatment of carbon nanotubes with conc. nitric acid. Pt particles with the average particle size of 4.9 nm are mostly distributed on the external surface of the CNTs (Fig. 1a) and slightly aggregated (Fig. 1b). Statistically, the Ru nanoparticle size was calculated to be ~3.5 nm (Fig. 1c). Some of Ru nanoparticles are also aggregated (Fig. 1d), which may have occurred during reduction of the catalysts due to the absence of any protective agent in the process.

The XRD pattern of Pt/CNTs is shown in Fig. 2a. The CNTs show typical diffraction peaks of (002) and (004) of graphite phase at 2θ = 26.0° and 42.8° respectively.[37] It also shows that the tubular graphite structure was not destroyed after conc. nitric acid treatment. The peaks at 2θ = 40.0°, 46.2°, 67.5° could be assigned respectively to the (111), (200) and (220) diffraction peaks of crystalline planes of cubic Pt (JCPDS No. 65-2868). All of these signal suggest that Pt was successfully deposited on CNTs. The average size of the Pt nanoparticles was calculated by the Scherrer equation, $D = 0.89\lambda/(\beta\cos\theta)$,[38] as 5.1 nm, in agreement with the result from TEM. For Ru/CNTs XRD pattern is shown in Fig. 2b. There is a distinct diffraction peak at 2θ = 22°, which is the carbon carrier characteristic diffraction peak, and the diffraction peaks at 2θ = 26.0°, 42.8° corresponding to the (002) and (004) crystal planes of the hexagonal graphite[37] (JCPDS NO. 41-1487). These data indicate that in the carbon nanotubes, the graphite layered structure has been retained. The XRD pattern of the Ru/CNTs catalyst does not show any peak for ruthenium metal

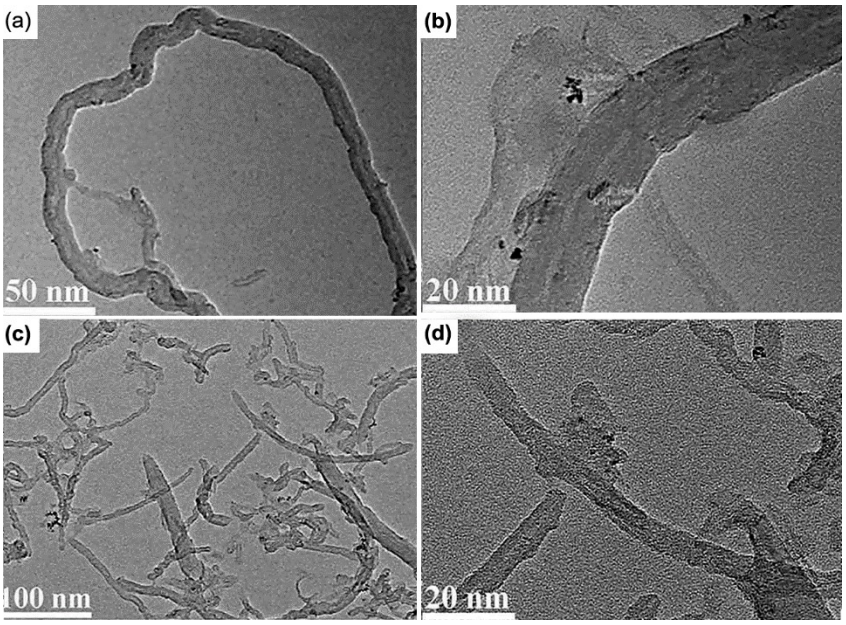

Fig. 1 — TEM images of (a & b) Pt/CNTs, and, Ru/CNTs (c & d).

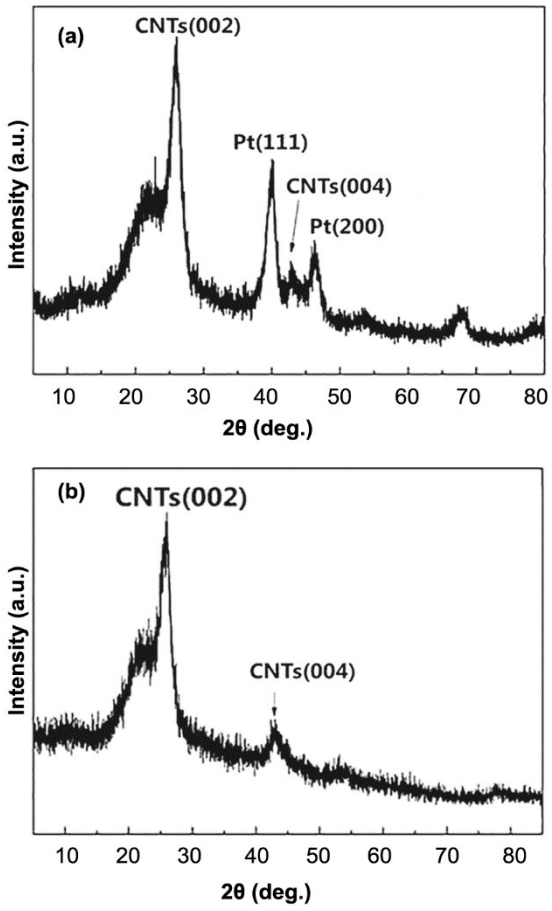

Fig. 2 — XRD patterns of (a) Pt/CNTs, and, (b) Ru/CNTs.

and its compounds, which may be because the Ru metal nanoparticles are better dispersed on the surface of carbon nanotubes, or that the diameter of the ruthenium nanoparticles is less than the detection limit of XRD (4nm).

Figure 3(a) shows the X-ray photoemission spectroscopy of Pt_{4f} in Pt/CNTs. The principle peaks at 71.4 eV and 74.7 eV are attributed to $Pt^0_{4f(7/2)}$ and $Pt^0_{4f(5/2)}$, while the peaks at 72.8 eV, 76.1 eV, 75.0 eV and 78.2 eV are assigned to Pt^{2+} and Pt^{4+}, respectively.[39] The relative intensity of different Pt species in Pt/CNTs is listed in Table 1. The relative intensity of Pt^0, Pt^{2+} and Pt^{4+} is calculated to be 51%, 43% and 6%, respectively. From the results we can conclude that most of the $(PtCl_6)^{2-}$ is reduced to Pt^0, although Pt^{2+} and Pt^{4+}, especially Pt^{2+} are also observed. The XPS diffraction pattern of Ru_{3p} in Ru/CNTs is shown in Fig. 3b. The diffraction pattern can be divided into peak and fitted to the figure. The binding energy position 462.5 eV peak is attributed to Ru^0, the binding energy at 463.9 eV peak to Ru^{3+} and the binding energy at 465.5 eV peak is attributed to Ru^{4+}, which coincides with the values reported in literature.[40] The relative intensity of the different Ru species in Ru / CNTs catalyst is shown in Table 1. It can be seen that the Ru^0, Ru^{3+} and Ru^{4+} are respectively 39%, 34% and 27%, indicating that most of the precursors are reduced to Ru^0, but there is still presence of the Ru^{3+} form. Compared to Pt reduction,

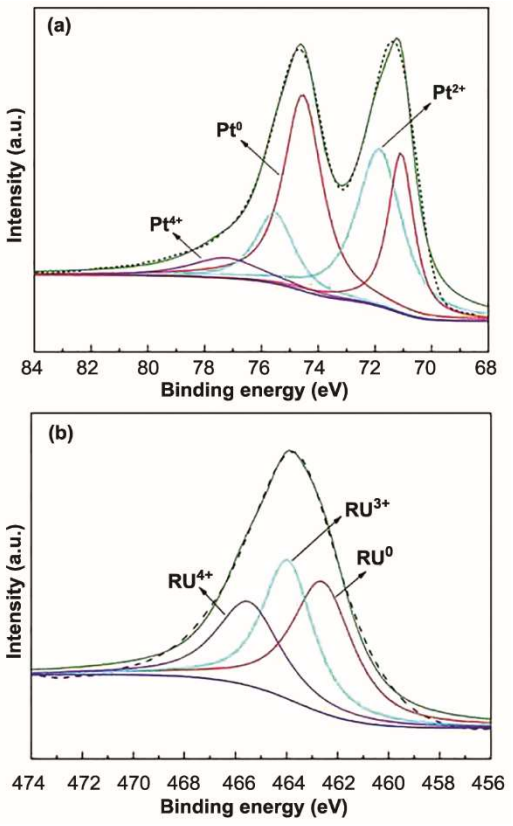

Fig. 3 — XPS spectra of Pt_{4f} in (a) Pt/CNTs, and, (b) Ru_{3p} in Ru/CNTs.

Table 1 — Relative intensity of different Pt species as observed from Pt_{4f} and Ru_{3p} spectra of Pt/CNTs and Ru/CNTs

Pt species	Rel. intensity (%)	Ru species	Rel. intensity (%)
Pt^0	51	Ru^0	39
Pt^{2+}	43	Ru^{3+}	34
Pt^{4+}	6	Ru^{4+}	27

the proportion of Pt precursors reduced to Pt^0 is greater than the proportion of Ru^0, which may be because the Pt reactivity is relatively weak and easily reducible.

The XPS spectrum of C_{1s} is given in Fig. 4a, showing different groups present in samples including the non-oxygenated ring C (C-C, 284.6 eV), the C in C-O bond (C-O, 286.6 eV) and the carbonyl C (C=O, 288.5 eV).[41] The relative intensity of the different carbon species obtained from the respective area is listed in Table 2, which shows that the surface functional groups of graphene in raw CNTs are changed after treatment with HNO_3. Many of oxygen-containing functional groups, e.g., hydroxyl and carbonyl groups, are introduced on the surface of CNTs, which could improve the adsorptivity of CNTs to the Pt nanoparticles. At the same time, the increase

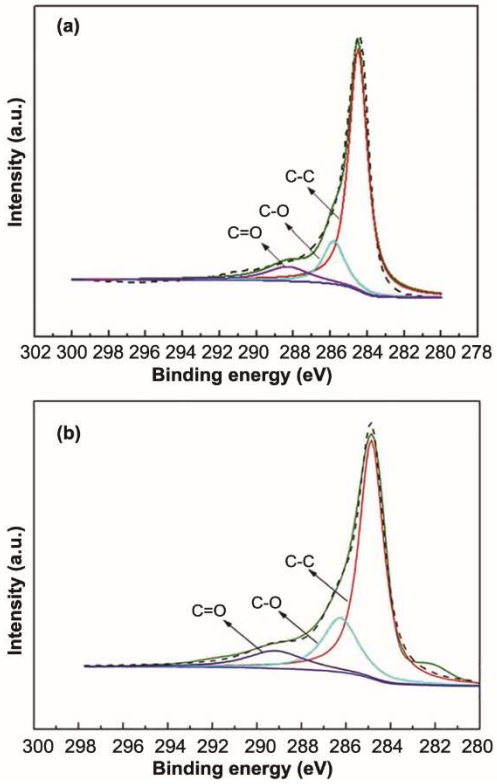

Fig. 4 — XPS spectra of C_{1s} in (a) Pt/CNTs, and, (b) Ru/CNTs.

Table 2 — Relative intensity of C species as observed from C_{1s} spectra of Pt/CNTs and Ru/CNTs

C species[a]	Rel. intensity (%)	C species[b]	Rel. intensity (%)
C-C	74	C-C	68
C-O	15	C-O	17
C=O	11	C=O	15

[a]Pt/CNTs. [b]Ru/CNTs.

in the amount of oxygen-containing groups would improve dispersity of Pt/CNTs in water. Figure 4b shows the XPS diffraction pattern of C_{1s} in Ru/CNTs catalyst. The position of the binding energy peak at 284.5 eV is attributed to C-C, while the peak at 285.8 eV peak is attributed to C-O and that at 288.3 eV peak to C=O. The relative intensity of the different carbon species obtained from the respective area is also listed in Table 2. It can be found from Table 2 that C-C, C-O and C=O contents are respectively 68%, 17% and 15%. This shows that the surface functional groups of carbon nanotubes are altered, which improves the adsorption capacity of carbon nanotubes for Ru, making it easier to form Ru supported on carbon nanotubes.

The nitrogen adsorption-desorption isotherm of Pt/CNTs is shown in Fig. 5a. The surface area, the

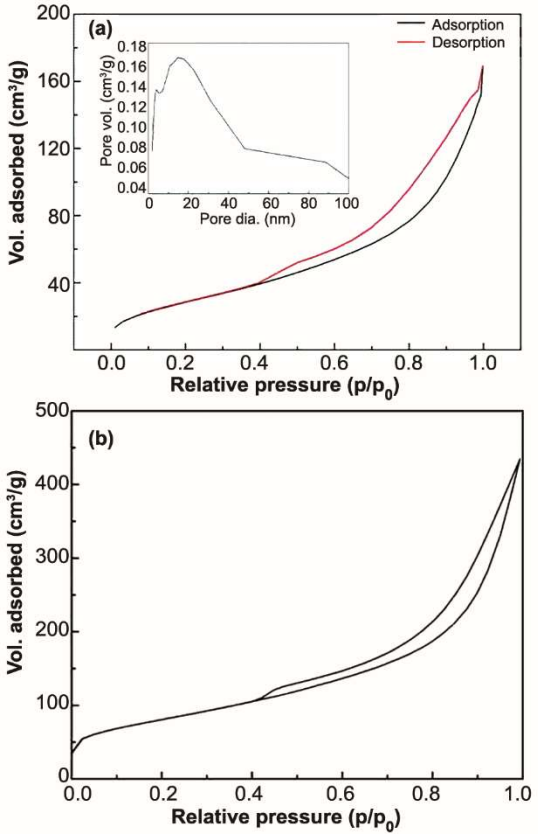

Fig. 5 — N_2 adsorption-desorption isotherms of (a) Pt/CNTs, and, (b) Ru/CNTs.

pore volume and the average pore diameter of Pt/CNTs are 108.65 m^2/g, 0.26 cm^3/g and 9.64 nm, respectively. From Fig. 5a we can see that the isotherm can be classified as type IV hysteresis loop according to IUPAC classification. In relation to the raw CNTs (outer diameter 20-30 nm), the surface area as well as the pore volume became smaller after the supporting of Pt nanoparticles. This may be due to the fact that some carrier pores are blocked after coating Pt metal salt.[42] Figure 5b depicts the Ru/CNTs catalyst nitrogen adsorption-desorption isotherm. The surface area, the pore volume and the average pore diameter of Pt/CNTs are 109.54 m^2/g, 0.31 cm^3/g and 8.65 nm, respectively. The pore volume is smaller than that of the pristine carbon nanotubes (181 m^2/g), which may be due to the loading of some Ru nanoparticles into the lumen of carbon nanotubes. Figure 5b shows the isotherm to be classified as the H4 type hysteresis loop.

The reusability of Pt/CNTs and Ru/CNTs were also investigated through the catalytic hydrogenation of *p*-methoxybenzaldehyde and acetophenone. After the first cycle of the hydrogenation was completed, the catalyst was filtrated out and washed with ethanol and deionized water for several times and dried in vacuum at 60 °C and used for the second cycle. Based on the conversion and selectivity results, it may be concluded that the catalyst exhibited promising reusability. There is no obvious loss of activity after each cycle. After the fourth cycle, the conversion of *p*-methoxybenzaldehyde and acetophenone remained relatively high, while there was no change in the selectivity (Supplementary data, Fig. 1).

In summary, carbon nanotubes supported Pt, Ru nanoparticles catalyst was prepared through an easy impregnation method. It is demonstrated that Pt/CNTs and Ru/CNTs are highly active and chemoselective catalysts for the aqueous-phase hydrogenation of aldehydes and substituted acetophenones. The use of water as the reaction medium makes these catalytic systems environmentally friendly.

Supplementary data

Supplementary data associated with this article are available in the electronic form at http://www.niscair.res.in/jinfo/ijca/IJCA_56A(12)1321-1326_SupplData.pdf.

Acknowledgment

This research was financially supported by NSFC (21163016, 21563026, and 21202133), Gansu Provincial Natural Science Foundation of China (1208RJZA287), and the Program for Changjiang Scholars and Innovative Research Team in University (IRT1177), PR China. We also thank the Key Laboratory of Eco-Environment- Related Polymer Materials (Northwest Normal University), Ministry of Education, PR China, for financial support.

References

1 Anastas P T & Farris C A, *Benign by Design* (American Chemical Society, Washington, USA) 1994, p. 212.
2 Trost B, *Science,* 254 (1991) 1471.
3 Trost B M, *Accounts Chem Res,* 35 (2002) 695.
4 Wender P A, Croatt M P & Witulski B, *Tetrahedron,* 62 (2006) 7505.
5 Li C J, *Chem Rev,* 105 (2005) 3095.
6 Grosselin J M, Mercier C, Allmang G & Grass F, *Organometallics,* 10 (1991) 2126.
7 Taylor A D, DiLeo G J & Sun K, *Appl Catal B: Environ,* 93 (2009) 126.
8 Welton T, *Chem Rev,* 99 (1999) 2071.
9 EARLE, J. M, SEDDON & R. K, *Ionic liquids. Green solvents for the future* (Pure and applied chemistry, Research Triangle Park, NC, ETATS-UNIS) 2000, p. 8.
10 Horváth I T, *Acc Chem Res,* 31 (1998) 641.

11 Shaughnessy K H, *ChemInform,* 37 (2006) 1827.
12 Li C J & Chen L, *ChemInform,* 37 (2006) 68.
13 Joo F, *ChemInform,* 33 (2002) 738.
14 Narayan S, Muldoon J, Finn M G, Fokin V V, Kolb H C & Sharpless K B, *Angew Chem Int Ed,* 44 (2005) 3275.
15 Wu X, Li X, King F & Xiao J, *Angew Chem,* 117 (2005) 3473.
16 Letondor C, Pordea A, Humbert N, Ivanova A, Mazurek S, Novic M & Ward T R, *J Am Chem Soc,* 128 (2006) 8320.
17 Eichenseer C M, Kastl B, Pericàs M A, Hanson P R & Reiser O, *ACS Sustainable Chem Eng,* 4 (2016) 2698.
18 Samec J S M, Baeckvall J E, Andersson P G & Brandt P, *ChemInform,* 37 (2006) 237.
19 Li J, Zhang Y, Han D, Jia G, Gao J, Zhong L & Li C, *Green Chem,* 10 (2008) 608.
20 Nait Ajjou A & Pinet J L, *J Mol Catal A: Chem,* 214 (2004) 203.
21 Melean L G, Rodriguez M, González A, González B, Rosales M & Baricelli P J, *Catal Lett,* 141 (2011) 709.
22 Marchetti M, Minello F, Paganelli S & Piccolo O, *Appl Catal A: Gen,* 373 (2010) 76.
23 Di Dio S, Marchetti M, Paganelli S & Piccolo O, *Appl Catal A: Gen,* 399 (2011) 205.
24 Aprile C, Garcia H & Pescarmona P P, *Synthesis and Characterization of Supported Chiral Catalysts* (John Wiley & Sons, NJ, USA) 2011, p. 177.
25 Garcia J, Gomes H T, Serp P, Kalck P, Figueiredo J L & Faria J L, *Carbon,* 44 (2006) 2384.
26 Zgolicz P D, Stassi J P, Yañez M J, Scelza O A & de Miguel S R, *J Catal,* 290 (2012) 37.
27 Cano M, Villuendas P, Benito A M, Urriolabeitia E P & Maser W K, *Mater Today Commun,* 3 (2015) 104.
28 Li X, Wei J, Chai Y & Zhang S, *J Colloid Interface Sci,* 450 (2015) 74.
29 Chen Z, Guan Z, Li M, Yang Q & Li C, *Angew Chem,* 123 (2011) 5015.
30 Tourani S, Khorasheh F, Rashidi A M & Safekordi A A, *J Ind Eng Chem,* 28 (2015) 202.
31 Karousis N, Tsotsou G E, Evangelista F, Rudolf P, Ragoussis N & Tagmatarchis N, *J Phys Chem C,* 112 (2008) 13463.
32 Zhu K N, Qin H Y, Liu B H & Li Z P, *J Power Sources,* 196 (2011) 182.
33 Guo S, Liew K Y & Li J, *J Am Oil Chem Soc,* 86 (2009), 1141.
34 Chen W, Pan X & Bao X, *J Am Chem Soc,* 129 (2007) 7421.
35 Ma H, Wang L, Chen L, Dong C, Yu W, Huang T & Qian Y, *Catal Commun,* 8 (2007) 452.
36 Chen X, Lou Z, Qiao M, Fan K, Tsang S C & He H, *J Phys Chem C,* 112 (2008) 1316.
37 Terrones M, Hsu W K, Schilder A, Terrones H, Grobert N, Hare J P, Zhu Y Q, Schwoerer M, Prassides K, Kroto H W & Walton D R M, *Appl Phys A,* 66 (1998) 307.
38 Tong H, Li H L & Zhang X G, *Carbon,* 45 (2007) 2424.
39 Xin Y, Liu J g, Zhou Y, Liu W, Gao J, Xie Y, Yin Y & Zou Z, *J Power Sources,* 196 (2011) 1012.
40 Xiong J, Dong X & Li L, *J Nat Gas Chem,* 21 (2012) 445.
41 Su C Y, Xu Y, Zhang W, Zhao J, Tang X, Tsai C H & Li L J, *Chem Mater,* 21 (2009) 5674.
42 Abbaslou R M M, Tavassoli A, Soltan J & Dalai A K, *Appl Catal A: Gen,* 367 (2009) 47